Frontiers | Frontiers in Marine Science

Effects of ammonia nitrogen stress on liver tissue structure and physiological indicators, and metabolomic analysis of juvenile four-finger threadfin (*Eleutheronema tetradactylum*)

Jing-Hui Jin[1], Hao-Jie Wang[1], Eric Amenyogbe[2], Yi Lu[1], Rui-Tao Xie[3], Zhong-Liang Wang[1,4,5] and Jian-Sheng Huang[1,4,5]*

[1]Fishery College, Guangdong Ocean University, Zhanjiang, China, [2]Department of Water Resources and Aquaculture Management, University of Environment and Sustainable Development, Somanya, Ghana, [3]Guangdong Evergreen Feed Industry Co. Ltd, Zhanjiang, China, [4]Guangdong Provincial Key Laboratory of Aquatic Animal Disease Control and Healthy Culture, Zhanjiang, China, [5]Guangdong Marine Fish Science and Technology Innovation Center, Zhanjiang, China

In intensive aquaculture, ammonia nitrogen (NH_3-N) is a major pollutant, causing oxidative stress and immune damage to aquatic organisms. The liver is crucial in protecting against biotic and abiotic stresses, but the response mechanisms to ammonia stress in juvenile four-finger threadfin (*Eleutheronema tetradactylum*) are not well understood. This study investigated these mechanisms by examining liver tissue structure, enzyme activities, and metabolomic changes in response to ammonia stress. Juvenile four-finger threadfin (7.4 ± 0.6 g) were divided into control, NH_3-N stress (50% LC_{50} 96_h, 10 ± 0.4 mg/L), and postexposure recovery groups. Stress durations of 12, 24, 48, and 96 h were evaluated, followed by 48 h recovery. Prolonged ammonia stress led to increased liver tissue damage, including disordered hepatocyte arrangement, swelling, necrosis, and the disappearance of nucleoli. After 48 h recovery, liver damage was alleviated but did not fully return to control levels, suggesting that the toxic effects of ammonia are recoverable yet persistent. Antioxidant enzyme activities (superoxide dismutase, catalase, and glutathione peroxidase) initially showed significant increases peaking at 24 h after stress, before declining by 96 h. Malondialdehyde levels rose initially and remained elevated compared with controls. After 48 h of recovery, antioxidant enzyme activity had not returned to control levels, indicating inadequate recovery from ROS-induced stress. Metabolomic analysis revealed 1219 significantly different metabolites in the 96 h stress group, with increases in $_L$-histidine, $_L$-threonine, and cholesterol. In the recovery group, 904 metabolites differed from controls, with notable reductions

in urea and choline. The key affected pathways included amino acid, lipid, and nucleotide metabolism. This study elucidates the toxic effects of ammonia nitrogen on juvenile four-finger threadfin and their adaptive responses through physiological and metabolomic changes, providing insights for aquaculture practices and breeding ammonia-tolerant strains.

1 Introduction

The four-finger threadfin (*Eleutheronema tetradactylum*) is a commercially important aquaculture species, valued for its high nutritional content and economic significance (Iqbal et al., 2023; Arief et al., 2023; Huang et al., 2022; Qu et al., 2020). It exhibits adaptability to a wide range of salinities and can be cultivated in seawater, brackish, or freshwater. With its fast growth rate and fresh, tender meat, the Food and Agriculture Organization has promoted *E. tetradactylum* as a key aquaculture species, with successful large-scale seedling production in Guangdong, China (Rainboth, 1996; Ou, 2017).

This species is primarily cultured in ponds; however, several issues arise in its culture, including the dissolution of residual bait, concentrated fish excretion, and excessive feeding. These factors contribute to eutrophication of breeding environments, leading to a rapid increase in metabolite and organic matter content, which can elevate aquatic ammonia nitrogen (NH₃-N) concentrations. Eutrophication is a process where water bodies, like lakes, ponds or rivers, become overly enriched with nutrients (such as nitrogen and phosphorus), often due to runoff from agricultural or urban areas (Wu, 2008). This nutrient overload stimulates excessive growth of algae, which can deplete oxygen levels in the water when the algae die and decompose, harming aquatic life. These conditions cause stress to the fish and adversely affect pond farming efficiency (Zhang et al., 2018). A critical environmental challenge in *E. tetradactylum* farming is the management of ammonia nitrogen (NH₃-N) concentrations, which can adversely affect fish health and growth (Jin et al., 2024; Lin et al., 2022; Zhang et al., 2018). Ammonia is a colorless, pungent gaseous compound of hydrogen and nitrogen (one nitrogen atom and three hydrogen atoms, NH₃) that is highly soluble in water. In water, it can exist as toxic un-ionized ammonia (NH₃) or less toxic ammonium ions (NH₄⁺), depending on the pH and temperature (Edwards et al., 2024; Xu et al., 2021). mg/L is a significant byproduct of animal waste and decomposition, agricultural runoff, industrial discharge, and aquaculture, exists as nonionized ammonia (NH₃) and ionized ammonium (NH₄⁺) Lin et al., 2022) and excessive levels can be harmful to aquatic organisms (Edwards et al., 2024). The safety limit of ammonia nitrogen concentration in marine aquaculture is 0.02 mg/L (Fishery Water Quality Standard, GB11607-89). High

NH₃-N levels can impair the physiological functions of *E. tetradactylum*. Effective management of ammonia levels is essential for the successful aquaculture of *E. tetradactylum* (Jin et al., 2024). The balance between these forms depends on pH, with NH₃ being highly toxic to aquatic organisms even at low concentrations (Edwards et al., 2024). High ammonia levels disrupt physiological homeostasis, affecting organ function and metabolic processes (Edwards et al., 2024; Ip and Chew, 2010). NH₃-N, which constitutes the majority of nitrogen metabolism in fish, can support aquaculture ecosystem stability at moderate levels but becomes harmful when excessive (Zhao et al., 2020). Its toxicity is influenced by water temperature and pH (Camargo and Alonso, 2006). The detrimental effects of NH₃-N on aquatic species include toxicity and immune suppression, as observed in *Oreochromis niloticus* (Qiang et al., 2011), *Mylopharyngodon piceus* (Hu et al., 2012), and *Hippoglossus hippoglossus* (Paust et al., 2011). Most bony fish are particularly sensitive (Handy and Poxton, 1993). The liver plays a key role in detoxifying NH₃-N but can suffer tissue damage when its metabolic capacity is exceeded (Mishra and Mohanty, 2008; Hargreaves and Kucuk, 2001).

Consequently, NH₃-N is a key constraint in the pond culture of this species as *E. tetradactylum* is particularly sensitive to environmental stressors such as NH₃-N. The liver is the central organ for detoxification and metabolism, making it vulnerable to ammonia toxicity (Mohiuddin and Khattar, 2023; Zeng et al., 2021), which can induce histopathological changes in liver tissue, alter physiological indicators, and disrupt metabolic pathways, ultimately impacting growth and survival (Zhou et al., 2023; Zhang et al., 2019). Histopathological refers to the microscopic study of tissue changes caused by disease or stress. In environmental studies, histopathological analysis is used to assess the impact of pollutants, like ammonia, on the tissues of aquatic organisms, providing insights into their health and environmental stress (Pramanik and Biswas, 2024; Ruiz-Picos et al., 2015). Anthropogenic pollutants are increasing in aquatic environments, with NH₃-N posing a significant threat to marine and freshwater organisms (Bănăduc et al., 2024; Lin et al., 2022; Bashir et al., 2020).

Despite the consequences of ammonia toxicity, studies integrating histological, physiological, and metabolomic analyses of ammonia stress on juvenile four-finger threadfin are lacking. This study addresses this gap by investigating the effects of NH₃-N stress

on liver tissue structure, physiological indicators, and metabolomics profiles. An NH_3-N stress test and recovery test were conducted to analyze the effects over 12, 24, 48, and 96 h, and with 48 h of recovery. Metabolomics, the comprehensive study of small molecules (metabolites) within biological systems, is particularly well-suited for this research due to the fact that metabolomics effectively reveals how ammonia nitrogen stress disrupts liver metabolism by detecting changes in metabolites and affected pathways, such as energy metabolism and antioxidant defense. It provides a holistic view of liver function, identifies potential biomarkers, and enhances understanding of stress and recovery when combined with physiological indicators. Using a multidisciplinary approach, this research aims to elucidate the mechanisms underlying ammonia-induced liver damage and provide effective strategies to mitigate the adverse effects of ammonia in aquaculture systems. This study also offers valuable insights for managing four-finger threadfin pond cultures and breeding for NH_3-N tolerance. Implementing appropriate water quality management practices can mitigate the adverse effects of ammonia toxicity, promoting healthier and more productive aquaculture systems.

2 Materials and methods

2.1 Experimental fish and feeding management

Experimental fish were derived from juveniles bred by the fish seed engineering and breeding team of the Fisheries College of Guangdong Ocean University, China, in the biological research base of Donghai Island. One thousand healthy individuals were randomly selected and transported to the Guangdong Evergreen Feed Industry Co., Ltd. breeding base, Zhanjiang, China, by a special fry transport vehicle. The fish were allowed acclimatized for two weeks. The two week fish acclimation period was chosen to allow the fish to recover from transport stress, adapt to the experimental system, and stabilize their physiological and behavioral responses. This duration is commonly used in aquaculture research and has been shown to provide sufficient time for most species to achieve homeostasis under controlled conditions. The breeding facility is an indoor 500 L breeding tank with a 24 h continuous inflatable microwater aquaculture system. The feeding water was natural seawater that has undergone sedimentation and sand filtration, and the experimental water meets the national fishery water quality standard (GB 11607-89). During the temporary maintenance period, the dissolved oxygen level was ≥ 5 mg/L, NH_3-N was 0.10 ± 0.03 mg/L, pH was 8.1 ± 0.2, water temperature was 28 ± 0.5°C and salinity was 28–30. Fish were fed daily at 8:00 and 17:00 with special formula feed. The feed ingredients are as follows: crude protein content ≥55%, crude fat content ≥8%, crude fiber content ≤3%, crude ash content ≤16%, calcium ≤4%, total phosphorus 1.5-3.0, lysine ≥2.5%, moisture ≤9%, fish and shrimp raw materials ≥85%., and feces and residual bait were cleaned 1 h after feeding. The experiment was started after 2 weeks of acclimation.

2.2 NH_3-N stress and recovery experiment

The experiment was conducted in 500 L aquaculture boxes, with ten juvenile fish per tank. Based on the acute toxicity test, NH_3-N at a 96 h LC50 of 20 mg/L was used for the experiment. A control group (CG) (0.10 ± 0.03 mg/L) was established, with 50% LC_{50} 96 h as the NH_3-N group (AG) (10 ± 0.4 mg/L). NH_3-N concentrations can vary significantly depending on the species, stocking density, feeding rates, water exchange, and system management practices. Usually, NH_3-N levels in well-managed systems are kept below 0.5 mg/L, but they can spike to 2-5 mg/L or higher during periods of overfeeding, high organic waste accumulation, or inadequate water exchange (Zhou and Boyd, 2015). The LC_{50} (96h) value provides a benchmark for assessing acute toxicity and the threshold beyond which fish survival rates drastically decrease (Katsiadaki et al., 2021). Choosing NH_3-N concentrations based on a percentage of LC_{50} 50% simulates sub-lethal stress conditions commonly encountered in poorly managed or intensive aquaculture systems, enabling a realistic evaluation of the species' physiological and metabolic responses. Following NH_3-N exposure, juvenile fish in the recovery group (RAG) were placed in the control group water for 48 h. Each group was run in three replicates, with 60 fish per replicate. In the AG group, the NH_3-N concentration was adjusted to the designed mass concentration by using a 10 g/L NH4Cl stock solution. The Nessler's reagent colorimetric method was used to measure the NH_3-N mass concentration in the water every 6 h; the mother liquor was replenished in a timely manner to maintain the initial concentration. The corresponding concentration of experimental water was completely replaced every 24 h. Before the formal experiment, the animals were starved for 24 h and during the experiment they received no food. The temperature, pH, dissolved oxygen, and salinity of the test water were maintained to match those used during the acclimation period.

Ten fish were randomly selected from each replicate for sampling at 12, 24, 48, and 96 h of NH_3-N stress and 48 h of recovery. After being anesthetized with 60 mg/L MS-222, liver tissue samples were collected on ice, washed with physiological saline, and fixed in a 4% paraformaldehyde solution for histological staining or collected in 1 mL centrifuge tubes. After being frozen in liquid nitrogen, these samples were transferred to a −80℃ ultra-low temperature freezer for enzyme activity and metabolomic analysis.

2.3 Fabrication and observation of liver tissue microsections

Paraformaldehyde-fixed livers were rinsed with water, dehydrated with 70–95% ethanol, and cleared with xylene. After paraffin embedding, the tissue was continuously sectioned with a Leica microtome at a thickness of 5–6 μm. H&E staining and neutral resin mounting were used to observe and take photos under an optical microscope (Nikon E80i microscope with the Nikon Y-TV55 imaging system).

2.4 Determination of antioxidant enzyme activities

For each group, three liver tissue samples were selected from each replicate for the determination of superoxide dismutase (SOD), catalase (CAT), glutathione peroxidase (GPx), and malondialdehyde (MDA) contents. The cryopreserved liver tissue was thawed and weighed accurately. Normal saline was added according to the ratio of weight (g): volume (mL) = 1:9. The frozen liver tissue was homogenized in an ice water bath for 3–5 min, and then centrifuged at 4℃ and 2500rpm for 10min. SOD, CAT, GPx, and MDA contents were assessed in liver tissues using specific assay kits provided by Nanjing Jiancheng Technology Co., Ltd. (http://www.njjcbio.com/). CAT activity was measured using the ammonium molybdate method, following the manufacturer's protocol. The amount of H_2O_2 decomposed by 1 μmol/mg of tissue protein per second was defined as one activity unit. GPx was determined by colorimetry by the nonenzymatic reaction deducted per milligram of protein per minute, and the GSH concentration in the reaction system was reduced by 1 μmol/L as an enzyme activity unit. The hydroxylamine method was used for SOD activity, with the enzyme amount corresponding to 1 mg tissue protein when the SOD inhibition rate was 50% in a 1 mL reaction solution defined as the SOD activity unit. The exact conditions under which enzyme assays (SOD, GPx, CAT) were performed are as follow: The liver tissue was accurately weighed, and pre-cooled physiological saline was added at a weight (g): volume (ml) ratio of 1:10. The mixture was processed using a high-speed grinder, then centrifuged at 2500rpm for 10 minutes. Subsequently, 50 μl of the supernatant was taken for determination (50-fold dilution). The corresponding SOD assay kit (Nanjing Jiancheng Bioengineering) was used. Relevant reagents and test samples were mixed, incubated at room temperature for 10 minutes, and subjected to colorimetric analysis at a wavelength of 550 nm using a 1 cm optical path cuvette with distilled water as the zero reference. For the GPx assay, the corresponding kit (Nanjing Jiancheng Bioengineering) was used. Relevant reagents and test samples were mixed, centrifuged at 3500 rpm for 10 minutes, and the supernatant was taken for color development. The color development reaction was carried out by mixing the reagents and allowing the samples to stand at room temperature for 15 minutes. The optical density (OD) of each tube was measured at 412 nm using a 1 cm optical path cuvette, with distilled water used to set the zero value. The CAT assay was conducted using the corresponding kit (Nanjing Jiancheng Bioengineering). Relevant reagents and test samples were mixed, and 200 μl of the reaction solution was placed into a 96-well plate. The absorbance of each well was measured at a wavelength of 405 nm using a microplate reader.

2.5 Metabolome analysis

2.5.1 Metabolite extraction and detection analysis

Liver tissues from six randomly selected fish from the CG, AG, and RAG were used for metabolomic sequencing. 100 ± 2 mg of samples were weighed into 2 mL Eppendorf (EP) tubes, 1 mL of tissue extract was added (methanol: chloroform = 3:1), ground twice in a tissue grinder (50 Hz, 60 s), ultrasonicated at room temperature for 30 min, and placed on ice for 30 min. It was then centrifuged at 12,000 rpm and 4℃ for 10 min. Then, 650 μL of the supernatant was transferred to a 2 mL centrifuge tube and concentrated in a vacuum concentrator until it was completely dry. Subsequently, 200 μL of 50% acetonitrile solution (v/v) was added to make 2-chlorophenylalanine solution (4 ppm) for reconstitution, followed by filtration; the filtrate was used for liquid chromatography–mass spectrometry (LC–MS) detection.

Chromatographic analysis was performed with the Thermo Vanquish instrument, Acquity UPLC HSS T31.8 μm (2.1 × 150 mm) chromatographic column. The autosampler performed a 2 μL gradient elution (temperature 8℃, flow rate 0.25 mL/min, column temperature 40℃), and the mobile phase was positive ions [0.1% formic acid water (B), 0.1% formic acid acetonitrile (A), and negative ions (5 mM ammonium formate water (B), acetonitrile (A)]. The gradient elution program was 0~1 min, 2% A; 1~9 min, 2~50% A; 9~12 min, 50~98% A; 12~13.5 min, 98% A; 13.5~14 min, 98~2% A; 14~20 min, 2% A-positive mode (14~17 min, 2% A-negative mode). In addition, 20 μL of each sample to be tested was mixed into a quality control sample to evaluate the LC–MS stability over the entire data collection process.

A Thermo Q Exactive Plus instrument was used for mass spectrometry in electrospray ion source (ESI), positive and negative ion ionization mode, with positive ion spray voltage of 3.50 kV, negative ion spray voltage of 2.50 kV, sheath gas 30 arbitrary units (arb), auxiliary gas 10 arb. The capillary temperature was 325℃, using full scan with a resolution of 70,000 and a scan range of 81~1000. Hot Compressive Dwell (HCD) was used for secondary cracking, with collision voltage of 30 eV, and dynamic exclusion to remove unnecessary MS/MS information. In addition, 20 μL of each sample to be tested was mixed into a quality control (QC) sample to evaluate the stability of the LC–MS during the entire data collection process.

2.5.2 Significant difference metabolite identification

SDM was performed based on the method described by Yang et al. (2022) with some modifications. The original data obtained were converted into mzXML format by Proteowizard software (v3.0.8789), and then the R package XCMS was used for peak identification, filtration, and alignment (Smith et al., 2006). The main parameters were bw=5, ppm=15, peakwidth=c(5,30), mzwid=0.015, mzdiff=0.01, method=centWave. A data matrix of information including mass to charge ratio (m/z), retention time, and intensity was obtained, and The results showed of precursor molecules obtained in positive and negative ion modes were imported into Excel for analysis and the data were compared after batch normalization. Finally, the metabolites were identified based on precise molecular weight (molecular weight error < 20 ppm), and metabolites were annotated for Metlin (http://metlin.scripps.edu), MoNA (https://mona.fiehnlab.ucdavis.edu//), and self-built data based on the MS/MS fragmentation mode.

The R package gmodels was used to perform a principal component analysis (PCA) on the data and the R language package ropls was used to perform supervised, orthogonal partial least squares discriminant analysis (OPLS-DA). Seven cross-validations were used to evaluate the robustness and predictive ability of the model to verify the reliability (Hao et al., 2019). The variable importance plot (VIP) of OPLS-DA and the *P*-value of the *t*-test from the univariate statistical analysis were combined to screen the significantly different metabolites between groups. The threshold value was VIP ≥ 1 and *t*-test $P < 0.05$. Finally, the differential metabolites were compared to the Kyoto Encyclopedia of Genes and Genomes (KEGG) database (http://www.kegg.jp/kegg/pathway.html) for pathway enrichment analysis (Liu et al., 2020).

2.6 Data analysis

The experimental data were analyzed using SPSS 22.0, and graphs were created using GraphPad Prism 8. Group differences were assessed using paired t-tests (the control and the NH$_3$-N group). A *p*-value > 0.05 indicated no significant difference, a *p*-value < 0.05 indicated a significant difference, and a *p*-value < 0.01 indicated a highly significant difference.

3 Results

3.1 Effects of NH$_3$-N stress and recovery on liver tissue structure

The hepatocytes in the control group were uniform in size, normal in morphology, neatly arranged, and had clear contours. The cell nuclei were arranged in the center of the cells, and the hepatic sinusoids had normal morphology and were clearly visible (Figure 1). After 12 h of NH$_3$-N stress, the hepatocytes swelled; the nuclei became enlarged, shifted, and deformed; and the cytoplasm became loose and transparent (Figure 1). After 24 h of NH$_3$-N stress, hepatocytes showed vacuolation and some were congested, the cell outlines were blurred, and sinusoids were dilated (Figure 1). After 48 h of NH$_3$-N stress, the hepatocytes were sparse while some were necrotic, dissolved, and had blurred outlines; the sinusoids were dilated; punctate lesions were formed; and lipid vacuolation occurred (Figure 1). After 96 h of NH$_3$-N stress, hepatocytes were severely vacuolated and necrotic, nucleoli were blurred or even disappeared, and cell outlines were not obvious (Figure 1). After 48 h recovery, hepatocytes became enlarged, vacuolated, and had blurred outlines, and sinusoidal dilation was slightly alleviated (Figure 1).
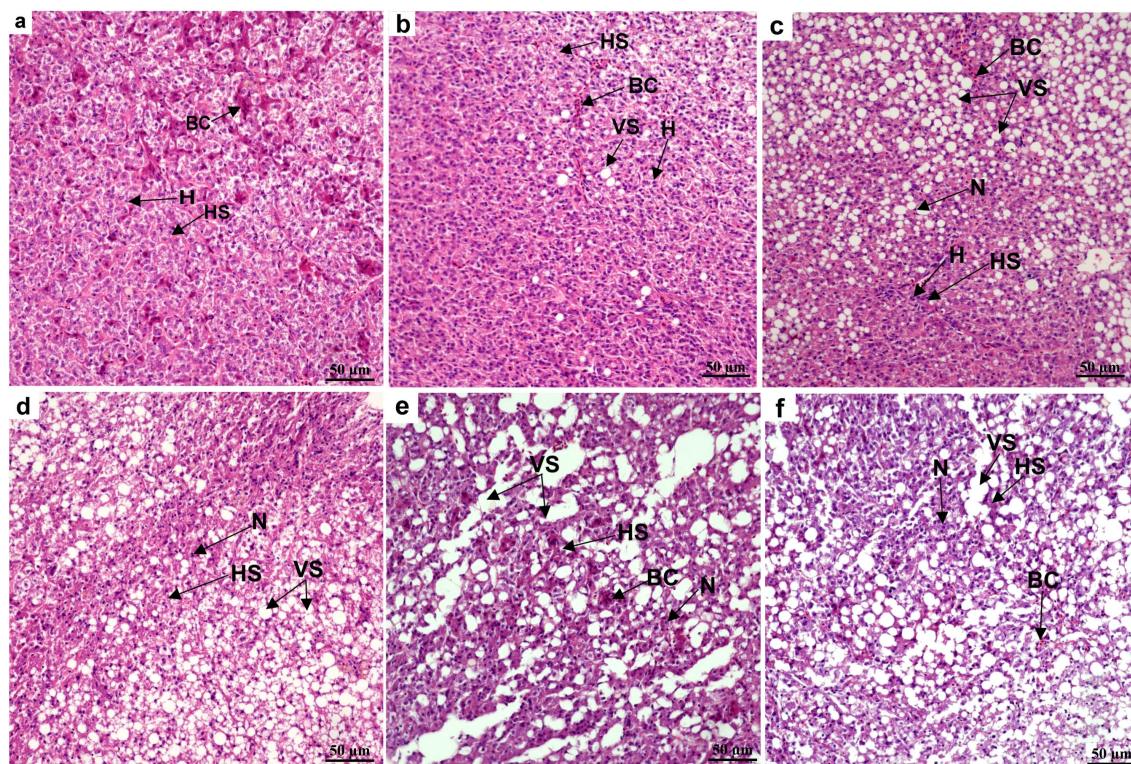
FIGURE 1
Effects of ammonia nitrogen exposure and its post-exposure recovery on liver microstructure in juvenile *E. tetradactylum*. **(A)** represents the microstructure of liver tissue of juvenile in control group; **(B–E)** respectively represents the microstructure of liver tissue of juvenile under ammonia nitrogen exposure (10 mg/L) for 12, 24, 48, 96 h; f respectively represents the microstructure of liver tissue of juvenile under post-exposure recovery for 48 h. BC, blood cells; H, hepatocyte; HS, hepatic sinusoid; N, nucleus; VS, vacuole structure; n = 9 per group.

3.2 Effects of NH₃-N stress and recovery on antioxidant enzymes

The effects of different NH₃-N exposure times on antioxidant enzyme activities in the liver tissue of juvenile four-finger threadfin are shown in Figure 2. After 12 h NH₃-N stress, SOD and CAT activities did not increase significantly compared with the control group ($P > 0.05$), while GPx increased significantly ($P < 0.01$). At 24 h of NH₃-N stress, the activities of SOD, CAT, and GPx increased compared with the control group, reaching highly significant levels ($P < 0.01$), and reached the highest peak at 24 h, and then showed a downward trend. After 48 h of NH₃-N stress, SOD and CAT activity both decreased significantly compared with the control group ($P < 0.05$ and $P < 0.01$, respectively), while GPx activity decreased but not significantly ($P > 0.05$). After 96 h of NH₃-N stress, SOD, CAT, and GPx activities were all significantly lower than in the control group ($P < 0.01$). During this period, SOD, CAT, and GPx activity first increased and then decreased. After 48 h of recovery, SOD, CAT, and GPx activity increased, but were still lower than in the control group, with SOD and CAT being highly significant lower compared with the control group ($P < 0.01$) and GPx being significantly lower ($P > 0.05$).

As NH₃-N exposure time increased, MDA content in the liver first increased and then decreased, with content at each time point being significantly higher than the control group ($P < 0.01$). After 48 h of recovery, the MDA content decreased although compared with the control group, it was significantly higher ($P < 0.05$).

3.3 Metabolome analysis

3.3.1 Sample quality and multivariate statistical analysis

LC–MS was used for untargeted metabolomic analysis, and the R language gmodels (v2.18.1) was used for PCA. The PCA score plot of the positive and negative ion modes shows that the QC samples were densely distributed, indicating that the data were reliable (Figure 3).

To maximize the screening of potential markers formed by intergroup differences, OPLS-DA models in positive and negative ion modes were established, and the model fitting ability was evaluated by Q2(cum), and R2Y(cum) (Figures 4, 5). There was an obvious separation between the positive and negative ion control group (CG) – the NH₃-N group (AG) and CG–RAG group in the OPLS-DA score graph. In the positive ion mode, the R2Y cumulative values of the OPLS-DA score graphs of the CG–AG group and the CG–RAG group were 1 and 0.999, respectively, and the Q2 values were 0.993 and 0.985, respectively (Figures 4A). In the negative ion mode, the cumulative values of R2Y were 0.999 and 0.999, and the values of Q2 were 0.993 and 0.986, respectively (Figures 5A). This shows that the OPLS-DA model had a good fit and therefore NH₃-N stress and recovery have a significant impact on the metabolism of liver tissue in four-finger threadfin. To verify the reliability of the OPLS-DA model, the two groups of models were cross-validated and permutation tested. In the positive and negative ion modes, Q2 and R2 were lower than the original values
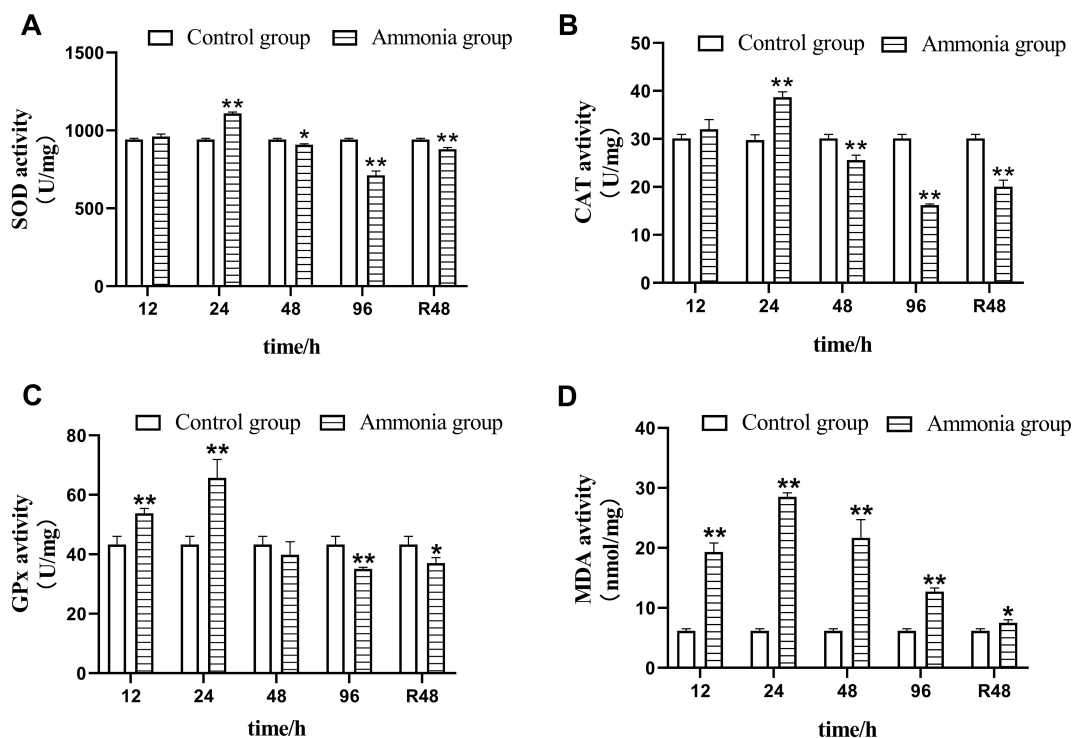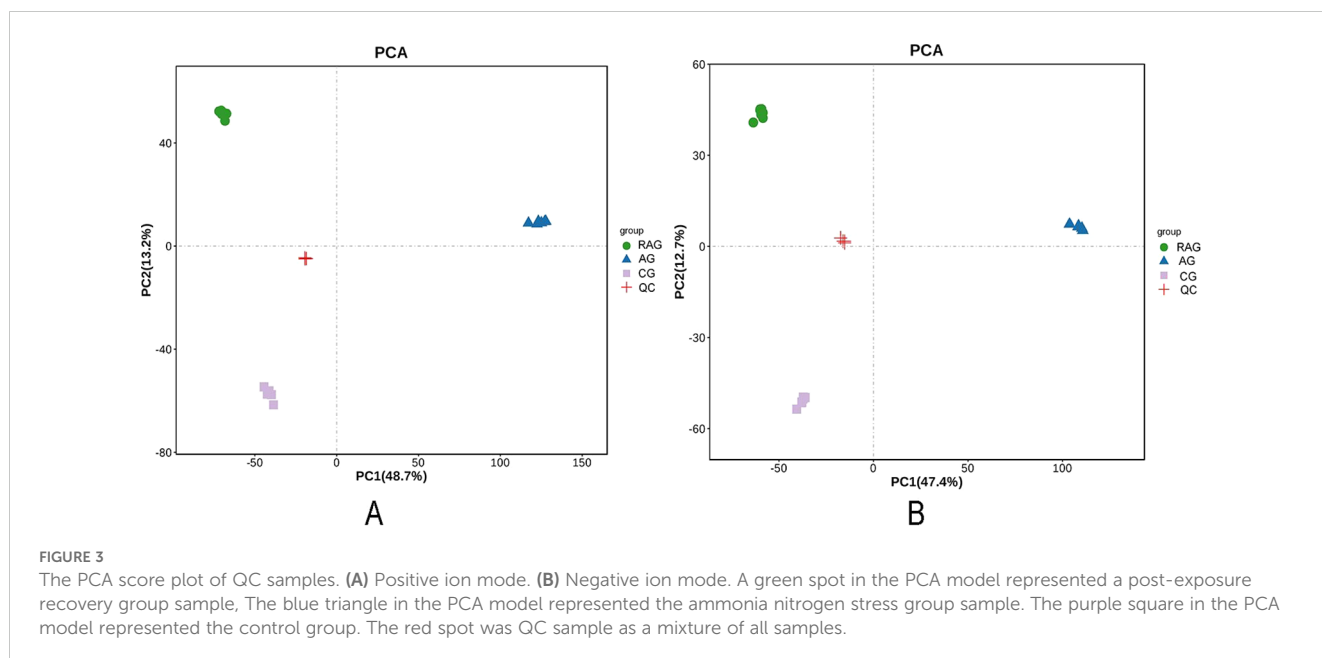

FIGURE 2
Effects of ammonia nitrogen exposure and its post-exposure recovery in liver antioxidant enzymes activities of juvenile *E. tetradactylum*. n = 9 per group.

FIGURE 3
The PCA score plot of QC samples. **(A)** Positive ion mode. **(B)** Negative ion mode. A green spot in the PCA model represented a post-exposure recovery group sample, The blue triangle in the PCA model represented the ammonia nitrogen stress group sample. The purple square in the PCA model represented the control group. The red spot was QC sample as a mixture of all samples.

from left to right, and the regression line of the point crossed the horizontal axis (Figures 4B, 5B, D); therefore, the model has reliable predictive ability and could be used for subsequent analysis.

3.3.2 Screening and identification of differential metabolites

To verify whether the differences in metabolites were significant, differential metabolites were screened based on the criteria of VIP ≥ 1 and t-test $P < 0.05$ in the OPLS-DA model, and the results from the drawing column chart are shown in Figure 6. In the CG–AG group, 1219 differential metabolites were screened, of which 248 were upregulated and 971 were downregulated. In the positive-ion mode, 123 of the differential metabolites were upregulated and 555 were downregulated. In the negative-ion mode, 125 of the differential metabolites were upregulated and 416 were downregulated. In the CG–RAG group, 904 differential metabolites were screened, of which 641 were upregulated and 263 were downregulated. In the positive-ion mode, 301 differential metabolites were upregulated and 171 were downregulated. In the negative-ion mode, 340 differential metabolites were upregulated and 92 were downregulated.

3.3.3 Analysis of differential metabolites and metabolic pathways

To explore the effect of NH₃-N exposure and postexposure recovery on metabolism, significant metabolites were further enriched by KEGG and the metabolic pathways were analyzed. The metabolites were mainly annotated into six major biological processes, including metabolism, genetic information processing, environmental information processing, cellular processes, organismal systems, and human diseases. The main metabolic pathways and signal transduction pathways involved in metabolites were global and overview maps, amino acid metabolism, chemical structure transformation maps, lipid metabolism, carbohydrate metabolism, metabolism of other amino acids, nucleotide metabolism, membrane transport, digestive system, and endocrine system. (Figure 7)

In the CG–AG group, a total of 163 pathways were enriched. The top 20 pathways enriched by KEGG are shown in Figure 8 and include ABC transport, pyrimidine metabolism, β-alanine metabolism, protein digestion and absorption, biotin metabolism, carbohydrate digestion and absorption, metabolic pathways, primary bile acid biosynthesis, tryptophan metabolism, etc. Among them, L-histidine, L-threonine, betaine, L-citrulline, taurocholic acid, and cholesterol increased, while glutathione, urea, adenosine, N-alpha-acetyl-L-ornithine, L-alanine, L-lysine, biotin, leucine, inosine, uridine, uracil, thymine, cytidine, and taurine decreased (Table 1).

In the CG–RAG group, a total of 155 pathways were enriched. The top 20 pathways enriched by KEGG are shown in Figure 8. The main enriched metabolic pathways include tryptophan metabolism, ABC transport, fatty acid degradation, lysine degradation, purine metabolism, metabolic pathways, linoleic acid metabolism, pyrimidine metabolism, amino acid biosynthesis, arginine and proline metabolism, etc. Among them, L-threonine, adenosine, betaine, L-alanine, uridine, cytidine, 5-hydroxy-L-tryptophan, leucine, phenylalanine, and adenine showed increased, while urea, choline, L-histidine, guanine, hypoxanthine, 5-aminopentanoic acid, creatinine, inosine, and thymine decreased (Table 2).

L-histidine is an essential amino acid that plays a key role in protein synthesis and serves as a precursor for the synthesis of histamine, an important neurotransmitter involved in immune response. Upregulation of L-histidine indicate an adaptive response to stress, potentially enhancing immune function or promoting tissue repair mechanisms in response to environmental stressors such as ammonia exposure. Conversely, a decrease in L-histidine levels suggest impaired growth or altered energy metabolism due to environmental challenges. The regulation of amino acids like L-histidine reflects the body's physiological response to stress.
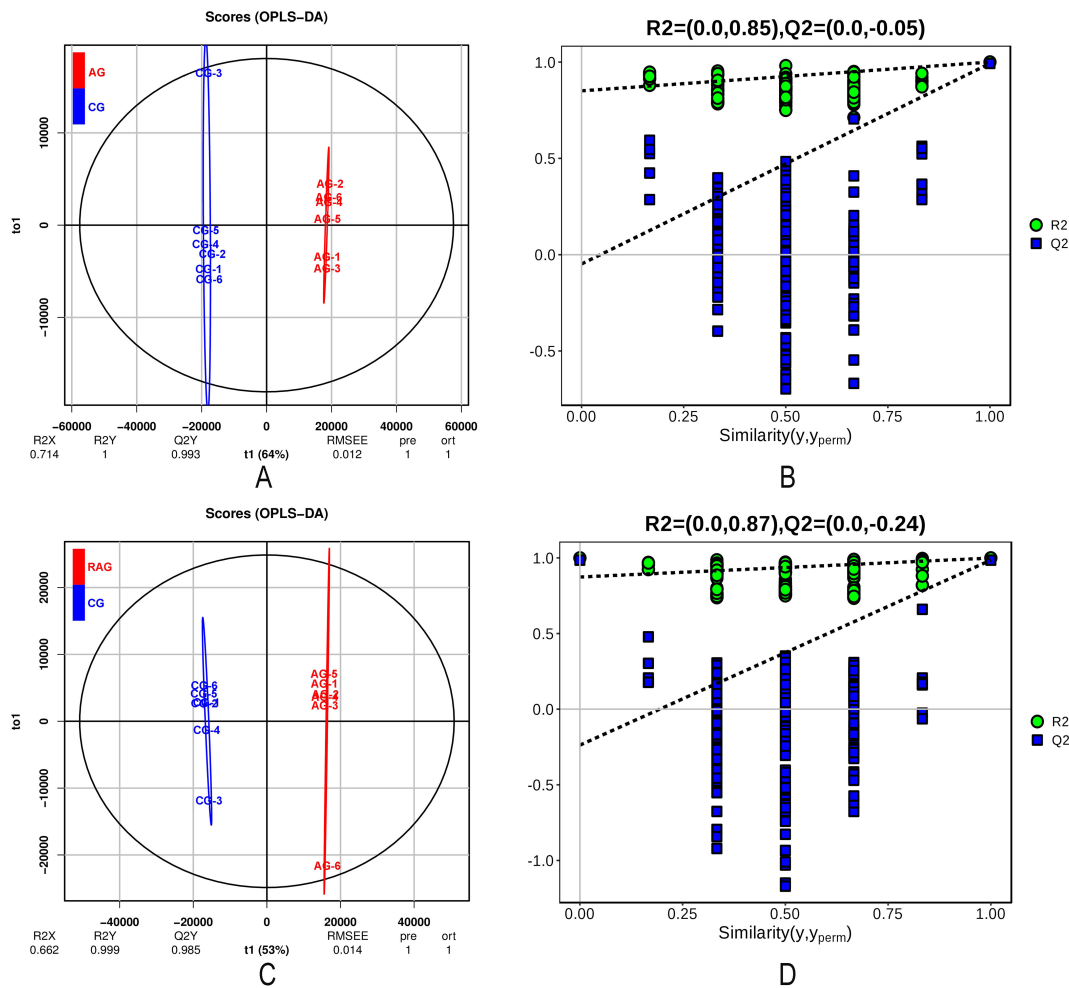
FIGURE 4
OPLS-DA model score diagram and OPLS-DA permutation test in positive ion mode. **(A)** blue spot in the OPLS-DA modes score diagram ammonia nitrogen stress group (AG) sample, red spot in the OPLS-DA modes score diagram control group (CG). **(B)** OPLS-DA permutation test model between AG and CG. **(C)** blue spot in the OPLS-DA modes score diagram post-exposure recovery group (RAG) sample, red spot in the OPLS-DA modes score diagram control group (CG). **(D)** OPLS-DA permutation test model between RAG and CG. R2 and Q2 were model validation parameters, which represented model interpretability and model predictability, respectively.

4 Discussion

4.1 Effects of NH₃-N on liver tissue structure

The study on NH₃-N stress in juvenile four-finger threadfin (*E. tetradactylum*) reveals significant impacts on liver tissue structure, antioxidant enzyme activity, and metabolic pathways. These findings align with and expand upon previous research on ammonia toxicity in aquaculture species. The liver is a key organ for metabolism and detoxification in fish, and ammonia nitrogen (NH₃-N) can reach the liver through the portal vein, participating in metabolic processes (Abbas, 2006). Excessive ammonia disrupts the balance between substance synthesis and release in hepatocytes, leading to cell vacuolation, edema, necrosis, and impaired liver function (Wen et al., 2019). Liver pathology, including vacuolation and necrosis, has been observed in fish exposed to NH₃-N, such as *Oreochromis niloticus* (Benli et al., 2008), *Megalobrama*

amblycephala (Zhang et al., 2015), and *Verasper variegatus* (Wang et al., 2017).

In this study, juvenile four-finger threadfin exposed to NH₃-N showed progressive liver damage. Control group liver tissue displayed a healthy architecture, serving as a baseline. After 12 h of NH₃-N exposure, hepatocytes swelled, nuclei enlarged and shifted, and cytoplasm loosened, indicating early oxidative damage and structural disintegration (Qiang et al., 2011; Molines et al., 2022). By 24 h, damage intensified with vacuolation, congestion, and sinusoidal dilation, reflecting compromised membrane integrity and lipid metabolism disruptions (Gómez-Virgilio et al., 2022; Safahieh et al., 2017). At 48 h, advanced necrosis, nuclear dissolution, and punctate lesions were evident, signaling overwhelmed cellular repair mechanisms and severe metabolic dysfunction (Yoon et al., 2021). By 96 h, liver tissue showed extensive vacuolation, widespread necrosis, and loss of structural integrity.

After 48 h of recovery, some repair occurred, with reduced sinusoidal dilation, though hepatocytes remained enlarged and
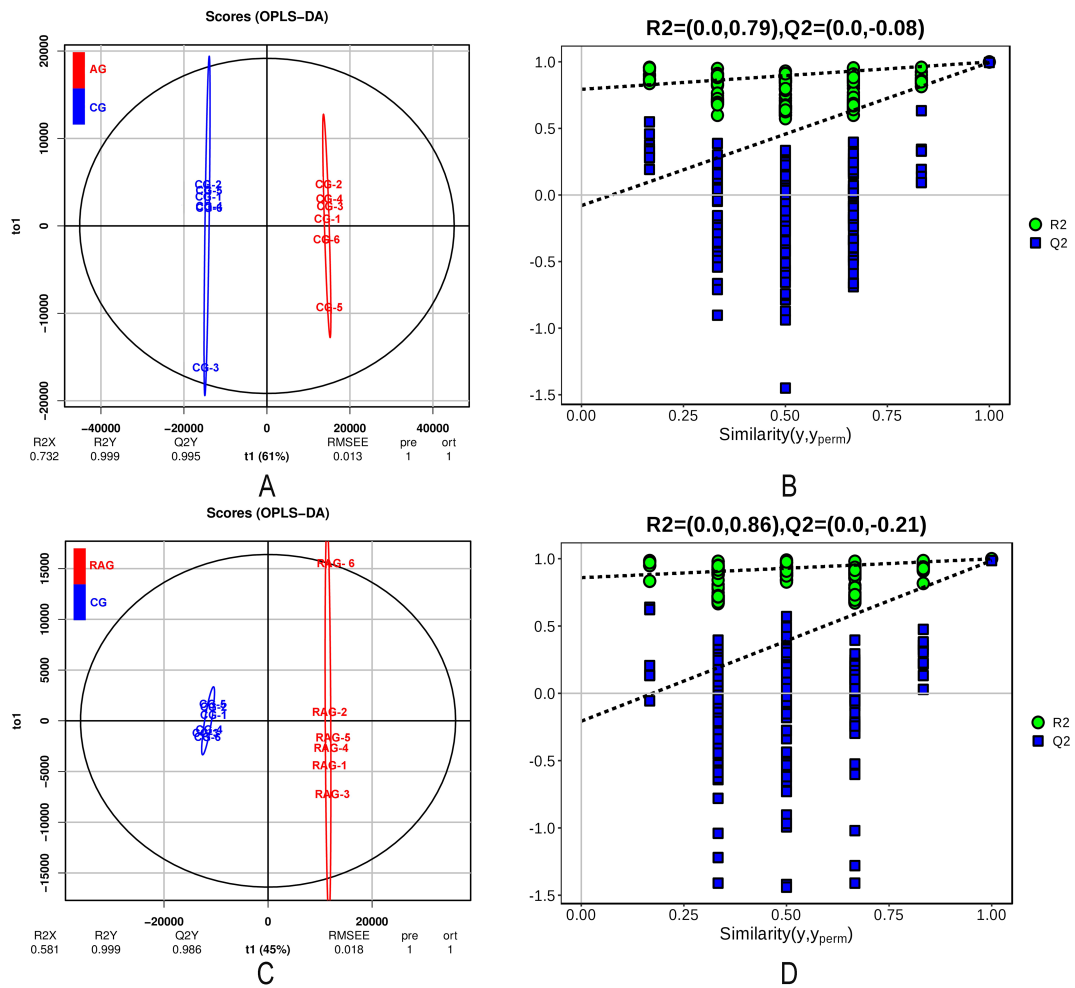
FIGURE 5
OPLS-DA model score diagram and OPLS-DA permutation test in negative ion mode. **(A)** blue spot in the OPLS-DA modes score diagram ammonia nitrogen stress group (AG) sample, red spot in the OPLS-DA modes score diagram control group (CG). **(B)** OPLS-DA permutation test model between AG and CG. **(C)** blue spot in the OPLS-DA modes score diagram post-exposure recovery group (RAG) sample, red spot in the OPLS-DA modes score diagram control group (CG). **(D)** OPLS-DA permutation test model between RAG and CG. R2 and Q2 were model validation parameters, which represented model interpretability and model predictability, respectively.
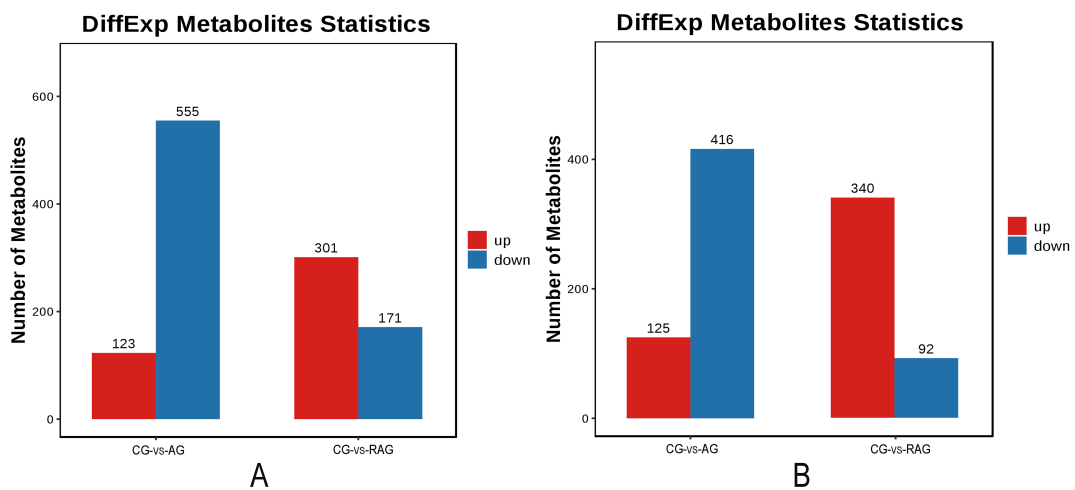
FIGURE 6
Statistical chart of the number of differential metabolites. **(A)** Positive ion mode. A red column chart represented a predominance up regulation metabolite. A blue column chart represented a predominance down regulation metabolite. **(B)** Negative ion mode.
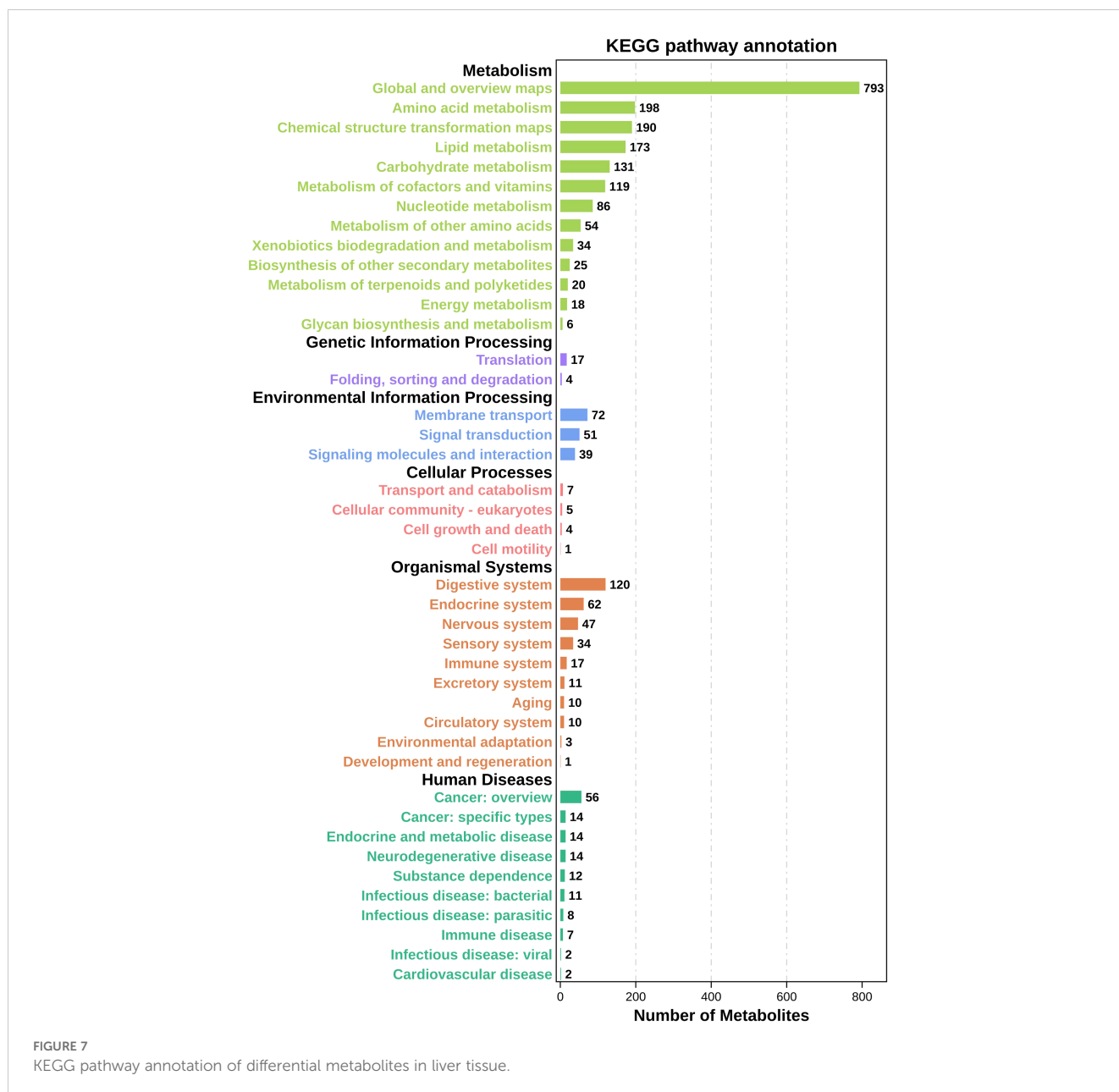
FIGURE 7
KEGG pathway annotation of differential metabolites in liver tissue.

vacuolated, indicating incomplete recovery (Figure 1). The persistent damage suggests potential long-term impacts on liver function, highlighting the need for optimal water quality in aquaculture to prevent NH₃-N accumulation and protect fish health.

Histopathological changes in the liver due to NH₃-N stress observed in this study mirror findings in species like Nile tilapia (*Oreochromis niloticus*) and grass carp (*Ctenopharyngodon idella*). Benli et al. (2008) and Zhang et al. (2015) reported similar hepatocyte vacuolation, necrosis, and sinusoidal dilation, suggesting a shared vulnerability among freshwater and brackish species to ammonia-induced hepatic damage. In contrast to these studies, the recovery period in the current research demonstrated partial tissue repair, indicating a potential for resilience in *E. tetradactylum*.

4.2 Effects of NH₃-N on antioxidant enzyme activities in liver tissue

When fish are subjected to NH₃-N stress, fish produce significant reactive oxygen species (ROS), triggering enzymatic and nonenzymatic antioxidant defense mechanisms, including superoxide dismutase (SOD), catalase (CAT), and glutathione peroxidase (GPx). SOD catalyzes the conversion of ROS to hydrogen peroxide (H_2O_2), which CAT and GPx further degrade into water and oxygen to maintain oxidative balance (Gao et al., 2015). A decrease in SOD activity signals reduced ROS elimination capacity (Liu et al., 2009). Malondialdehyde (MDA), a lipid peroxidation marker, reflects oxidative damage severity and antioxidant capacity (Du et al., 2016).

FIGURE 8
Top 20 of KEGG enrichment in liver tissue. **(A)** CG-AG group, **(B)** CG-RAG group.
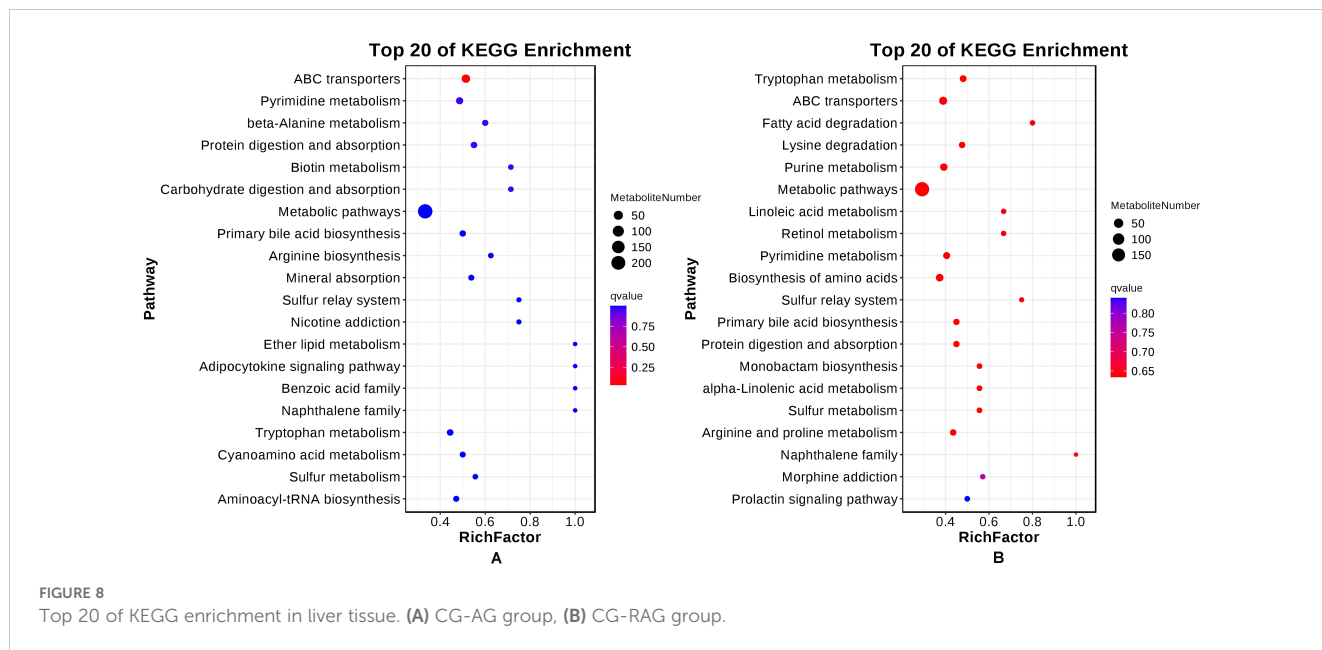
TABLE 1 Key differential metabolites screened between NH_3-N exposure and control groups.

ID	Name	Log$_2$FC	P-value	VIP	Trend
M325T382_POS	Glutathione	−4.6556	0.0000	1.435852	Down
M246T422_POS	Arg-Ala	−3.7818	0.0000	10.1279	Down
M121T115_POS	Urea	−0.6388	0.0000	2.261496	Down
M156T424_POS	L-Histidine	0.5705	0.0000	3.098542	Up
M120T358_2_POS	L-Threonine	0.6067	0.0000	1.536544	Up
M268T169_2_POS	Adenosine	−0.9165	0.0000	1.778781	Down
M118T268_2_POS	Betaine	0.4689	0.0000	4.718534	Up
M176T383_POS	L-Citrulline	0.3934	0.0000	1.937288	Up
M175T386_POS	N-alpha-acetyl-L-ornithine	−1.4009	0.0098	3.444227	Down
M466T196_POS	Cholesterol	0.5730	0.0041	2.446334	Up
M88T392_NEG	L-Alanine	−0.7039	0.0000	1.844604	Down
M145T547_NEG	L-Lysine	−0.8915	0.0000	1.519814	Down
M243T406_NEG	Biotin	−1.3532	0.0000	1.363044	Down
M130T257_2_NEG	Leucine	−1.4848	0.0000	18.7434	Down
M267T212_NEG	Inosine	−0.8771	0.0000	6.882785	Down
M243T387_NEG	Uridine	−1.5010	0.0000	1.325969	Down
M111T90_2_NEG	Uracil	−0.1363	0.0039	3.067979	Down
M125T79_2_NEG	Thymine	−1.8483	0.0000	5.426978	Down
M242T381_NEG	Cytidine	−0.1759	0.0000	1.04926	Down
M124T288_NEG	Taurine	−0.3100	0.0000	8.778179	Down
M164T251_NEG	Phenylalanine	−2.2911	0.0000	12.9816	Down
M146T374_2_POS	Acetylcholine	0.1734	0.0053	8.5272	Up
M258T382_1_POS	Glycerophosphocholine	−0.0919	0.0000	5.9917	Down
M1030T190_NEG	Taurocholic acid	3.0882	0.0000	3.9914	Up

TABLE 2 Key differential metabolites screened between the postexposure recovery and control groups.

ID	Name	Log$_2$FC	P-value	VIP	Trend
M121T115_POS	Urea	−1.3945	0.0000	3.4651	Down
M104T271_2_POS	Choline	−0.2245	0.0000	9.9475	Down
M156T424_POS	L-Histidine	−0.1707	0.0251	1.3727	Down
M120T358_2_POS	L-Threonine	1.2995	0.0000	2.9187	Up
M268T169_2_POS	Adenosine	0.2282	0.0001	1.1501	Up
M118T268_2_POS	Betaine	0.7129	0.0000	6.9795	Up
M152T226_2_POS	Guanine	−0.5111	0.0000	3.2668	Down
M137T168_2_POS	Hypoxanthine	−0.7285	0.0000	17.7766	Down
M100T28_POS	5-Aminopentanoic acid	−0.7151	0.0462	1.9270	Down
M114T169_2_POS	Creatinine	−0.5843	0.0000	3.6098	Down
M88T392_NEG	L-Alanine	0.2438	0.0000	1.5200	Up
M267T212_NEG	Inosine	−0.7190	0.0000	7.9977	Down
M243T387_NEG	Uridine	0.5280	0.0000	1.3549	Up
M242T381_NEG	Cytidine	0.2309	0.0000	1.6204	Up
M125T79_2_NEG	Thymine	−0.4636	0.0000	4.1621	Down
M219T408_NEG	5-hydroxy-L-tryptophan	0.6006	0.0000	1.9702	Up
M130T257_2_NEG	Leucine	0.2356	0.0000	11.9835	Up
M124T288_NEG	Taurine	0.1049	0.0004	6.3433	Up
M164T251_NEG	Phenylalanine	0.3223	0.0000	9.0296	Up
M134T160_NEG	Adenine	0.5607	0.0000	2.4298	Up
M367T483_POS	Phosphocholine	1.4206	0.0000	1.3940	Up
M279T47_NEG	Linoleic acid	−0.8592	0.0014	14.3046	Down
M279T53_POS	Gamma-linolenic acid	−0.8677	0.0038	1.3991	Down
M735T147_POS	1,2-dihexadecanoyl-sn-glycero-3-phosphocholine	−0.0808	0.0269	1.6692	Down

NH$_3$-N stress significantly impacted the antioxidant enzymes (SOD, CAT, and GPx) and lipid peroxidation (MDA content) in the liver of juvenile four-finger threadfin. Antioxidant activities initially increased but declined under prolonged exposure. After 12 h, SOD and CAT activity showed no significant change, while GPx activity increased, indicating its sensitivity to ROS-induced stress. At 24 h, all enzyme activities peaked, reflecting a full antioxidant response (Sun et al., 2024; Li et al., 2015; Hegazi et al., 2010). By 48 h, SOD and CAT activities declined significantly, and GPx decreased slightly. At 96 h, enzyme activities fell below control levels, suggesting oxidative damage (Bizoń et al., 2023). Post-recovery (48 h), enzyme activities improved but remained suboptimal, indicating residual stress effects. The antioxidant response showed a biphasic trend: early upregulation (12–24 h) followed by suppression (48–96 h) due to prolonged stress.

MDA levels, indicative of lipid peroxidation, increased significantly during NH$_3$-N exposure, reflecting oxidative damage from excessive ROS and overwhelmed antioxidant defenses.

Although recovery for 48 h led to a decrease, MDA levels remained higher than controls, underlining incomplete oxidative damage reversal (Colares et al., 2021). Prolonged NH$_3$-N stress caused oxidative damage, with increased MDA and diminished antioxidant enzyme activities, indicating limited hepatic capacity to manage sustained oxidative stress (Yan et al., 2023; Liu et al., 2021; Li et al., 2015). Antioxidant enzyme activities partially recovered after 48 h, but full liver recovery was not achieved. During 96 h of exposure, SOD, CAT, and GPx activities initially rose (12–48 h) due to ROS-triggered antioxidant defenses but later declined (48–96 h) as prolonged stress impaired enzyme function. This underlines the limited capacity of juvenile four-finger threadfin to withstand extended environmental stress.

Reactive oxygen species (ROS) accumulation is a hallmark of ammonia nitrogen (NH$_3$-N) stress. In this study, juvenile four-finger threadfin demonstrated a biphasic response in antioxidant enzyme activities under NH$_3$-N exposure. Initial exposure triggered upregulation of superoxide dismutase (SOD), catalase (CAT), and

glutathione peroxidase (GPx), peaking at 24 hours, followed by a decline as oxidative damage persisted. The rise in malondialdehyde (MDA) levels, indicative of lipid peroxidation, paralleled the decline in enzymatic activity, highlighting insufficient antioxidant defenses to counter sustained ROS attack. The biphasic response of superoxide dismutase (SOD), catalase (CAT), and glutathione peroxidase (GPx) activities to ammonia stress aligns with observations in *Siniperca chuatsi*, *Macropterus salmoides* and *Takifugu rubripes* (Liu et al., 2019; Zheng et al., 2020; Gao et al., 2021). While initial increases in enzyme activity reflect an adaptive response to oxidative damage, the subsequent decline underscores the limited capacity of antioxidant systems under prolonged stress. Similar trends in malondialdehyde (MDA) accumulation highlight persistent oxidative damage, emphasizing the need for managing NH₃-N levels to sustain antioxidant defenses. This enzymatic response mirrors findings in other species like *Oreochromis niloticus* and *Megalobrama amblycephala*, where prolonged ammonia exposure overwhelmed antioxidant systems, leading to oxidative damage and impaired liver function. NH₃-N exposure significantly elevates MDA levels in fish liver, as reported for *Dicentrarchus labrax* (Sinha et al., 2015), *Pelteobagrus fulvidraco* (Zhang et al., 2016), and *Verasper variegatus* (Wang et al., 2017). In this study, MDA levels in four-finger threadfin initially rose and then decreased during 96 h of NH₃-N exposure, remaining significantly higher than controls ($P < 0.01$). This highlights tissue membrane lipid oxidation under stress. Short-term exposure triggered antioxidant defenses, but prolonged stress led to oxidative damage, with only partial recovery after 48 h. The persistent elevation of MDA during recovery further underscores the incomplete repair of oxidative damage within 48 hours, suggesting that recovery time may be insufficient to fully restore antioxidant balance. These findings are vital for managing aquaculture stressors to protect juvenile four-finger threadfin.

4.3 Effects of NH₃-N on metabolomics in liver tissue

NH₃-N stress and recovery significantly affect liver metabolism in juvenile four-finger threadfin, as evidenced by robust metabolomic data and validated OPLS-DA models. Using VIP ≥ 1 and $P < 0.05$ as criteria, 1219 differential metabolites were identified in the CG–AG group (248 upregulated, 971 downregulated), while 904 were found in the CG–RAG group (641 upregulated, 263 downregulated). KEGG enrichment revealed 163 pathways in the CG–AG group and 155 in the CG–RAG group. NH₃-N stress caused pronounced metabolic alterations, with most metabolites downregulated. Recovery led to significant upregulation, indicating partial reversibility. These metabolites may serve as biomarkers for assessing fish under environmental stress. Further targeted analyses are needed to clarify the metabolic pathways and their relevance to fish health and aquaculture.

The liver is central to energy storage and conversion in fish, with amino acids often prioritized over glucose as an energy source under optimal conditions (Kullgren et al., 2013). Stress from environmental factors increases energy demands for homeostasis (Sokolova et al., 2012). Amino acids, vital for various physiological functions, can indicate ROS-induced stress (Yan et al., 2020). High NH₃-N exposure disrupts amino acid metabolism, leading to oxidative damage and metabolic responses, including changes in amino acids, glucose, ATP, and other metabolites (Zhang et al., 2013; Li et al., 2016; Ye et al., 2018). In this study, 96-hour NH₃-N exposure followed by 48-hour recovery altered amino acid pathways, including tryptophan and arginine metabolism. During exposure, L-histidine, L-threonine, and L-citrulline increased, while arginine, phenylalanine, and leucine decreased, reflecting disrupted energy metabolism and oxidative damage. Recovery led to the normalization of amino acid metabolism, with key changes in leucine and other metabolites. Leucine, critical for tissue repair and ATP production, may play a role in mitigating NH₃-N-induced bioenergetic disruption (Yang et al., 2014; Albrecht, 2007). Metabolomic profiling revealed significant shifts in amino acid, lipid, and nucleotide metabolism under ammonia stress, which corroborates findings in zebrafish (*Danio rerio*) and large yellow croaker (*Larimichthys crocea*) (Zhang et al., 2023; Qiu et al., 2018). For instance, the upregulation of L-histidine and downregulation of leucine under stress conditions parallels disruptions in energy and protein metabolism observed in other fish species. However, the study's recovery data demonstrated a partial normalization of metabolic profiles, a novel insight into the resilience of *E. tetradactylum* compared to species like Atlantic salmon (*Salmo salar*), which exhibit prolonged recovery periods (Sokolova et al., 2012). Lipid metabolites such as linoleic and γ-linolenic acids were downregulated during NH₃-N stress, reflecting their utilization in combating oxidative damage and maintaining energy balance (Fortin et al., 2017). Recovery saw partial restoration, with some lipid metabolites upregulated, indicative of ongoing membrane repair and cellular energy restoration. Comparable findings in *Dicentrarchus labrax* and *Verasper variegatus* suggest lipid metabolism as a central pathway in mitigating ammonia toxicity

Lipid metabolism is a key regulatory pathway for aquatic animals under environmental stress, supplying essential fatty acids, energy, and supporting immune responses (Lee et al., 2018). In this study, ammonia exposure induced ROS-induced stress in juvenile four-finger threadfin, altering lipid metabolism. Upregulation of acetylcholine and sulfocholic acid suggested a metabolic response to alleviate stress, while downregulation of glycerophosphocholine (GPC) and taurine indicated cell membrane damage (Baliou et al., 2020). Metabolites were enriched in primary bile acid biosynthesis and linoleic acid pathways (Figure 8). During recovery, upregulation of taurine and choline phosphate highlighted self-repair processes, while downregulation of choline, linoleic acid, γ-linolenic acid, and 1,2-hexadecanoyl-sn-glycerol-3-phosphate reflected incomplete recovery (Xu et al., 2022). Reduced GPC post-exposure suggested immune suppression and compromised health (Konger et al., 2008; Sahu et al., 2012). Downregulated linoleic and α-linolenic acid after recovery pointed to ongoing oxidative stress and disrupted biofilm composition (Furumoto et al., 2016). The observed alterations in

lipid metabolism, including downregulated glycerophosphocholine and linoleic acid pathways, are consistent with findings in grass carp under similar stress (Zhao et al., 2020). These changes indicate compromised membrane integrity and increased oxidative susceptibility. However, the upregulation of repair-associated metabolites like taurine during recovery highlights potential targets for enhancing stress tolerance.

Nucleotides and their derivatives are essential for biological processes, including nucleic acid synthesis, energy metabolism, and stress response (Lane and Fan, 2015). In the CG–AG group, metabolites such as guanosine, inosine, uridine, uracil, thymine, and cytidine were significantly downregulated, while betaine was upregulated. In the CG–RAG group, adenosine, uridine, cytidine, and betaine increased, while guanine, hypoxanthine, inosine, and thymine decreased, suggesting involvement in nitrogen degradation and anti-inflammatory effects (Ren and Pan, 2014). Purine biosynthesis relies on amino acids for energy, and the depletion of nucleotide precursors impairs energy metabolism (Yang et al., 2020). Reduced adenine, adenosine, and hypoxanthine levels suggest NH$_3$-N stress disrupts DNA/RNA biosynthesis, affecting protein synthesis. Nucleotides function as antioxidants, mitigating ROS-induced stress (Rébeillé et al., 2007). Betaine, upregulated after 96 h of NH$_3$-N stress, helps counter oxidative damage and supports membrane repair (Annunziata et al., 2019). Nucleotide metabolism was significantly altered under NH$_3$-N exposure, with downregulation of critical metabolites like adenosine, guanine, and thymine. These changes indicate impaired DNA and RNA synthesis, potentially affecting protein synthesis and cellular repair mechanisms. During recovery, partial upregulation of nucleotides such as cytidine and uridine suggests activation of reparative pathways. Similar nucleotide responses have been observed in stress studies on *Takifugu rubripes*. This study corroborates findings in other fish species, reinforcing the conserved biochemical responses to NH$_3$-N stress. In both freshwater and marine species, ROS-mediated oxidative damage, lipid peroxidation, and disruptions in amino acid and nucleotide metabolism are consistent outcomes of ammonia exposure. However, the degree of recovery varies, likely influenced by species-specific resilience and environmental conditions. The persistent impact of NH$_3$-N on liver function and metabolic pathways underscores the importance of maintaining optimal water quality in aquaculture systems.

ABC transporters are transmembrane proteins that utilize ATP hydrolysis to facilitate substance exchange and maintain cellular ion homeostasis (Andolfo et al., 2015). They play roles in nutrient absorption, toxin defense, and physiological functions like lipid transport, cell differentiation, and antigen presentation (Winston and Theriot, 2020). These transporters handle biomolecules such as amino acids, nucleotides, and peptides (Wilkens, 2015). In the CG–AG group, metabolites enriched in the ABC transport pathway, like glutathione and urea, were downregulated, while L-histidine and L-threonine were upregulated. In the CG–RAG group, urea and L-alanine were downregulated, with L-threonine significantly upregulated, showing NH$_3$-N stress and recovery affect liver transport equilibrium in four-finger threadfin. The CG–AG group displayed metabolic suppression, suggesting stress-induced shutdown or damage, whereas the CG–RAG group exhibited a stronger adaptive response during recovery. NH$_3$-N stress significantly alters key metabolic processes, likely to detoxify ammonia or mitigate its effects (Zhang et al., 2023). Disruptions in transcriptional and translational pathways could indicate adjustments in protein synthesis for stress management (Qiu et al., 2018). Liver cells likely regulate ion transport to maintain homeostasis (Aranda-Morales et al., 2021), with broader impacts on signaling, digestion, and growth (Han et al., 2021). These stress responses, including ROS-induced stress and inflammation, appear conserved across species (Ngo and Duennwald, 2022). The findings provide critical insights for aquaculture, emphasizing the importance of maintaining optimal NH$_3$-N concentrations to prevent chronic stress and its gushing effects on health and growth. The recovery dynamics observed in this study suggest that with appropriate interventions, such as enhanced water quality management and dietary supplementation, the resilience of *E. tetradactylum* can be leveraged to improve aquaculture sustainability.

5 Conclusions

Juvenile four-finger threadfin (*Eleutheronema tetradactylum*) exposed to ammonia nitrogen (NH$_3$-N, 10 ± 0.4 mg/L) for 96 hours exhibited significant liver tissue damage, including vacuolation, dilated sinusoids, necrosis, and blurred cell outlines, which intensified over time. Histopathological changes such as hepatocyte swelling, nuclear deformation, and dissolution reflected the progressive impact of ammonia toxicity. A 48-hour recovery period showed partial improvement, yet persistent hepatic damage suggested long-term effects on liver health and fish viability. Exposure to ammonia nitrogen triggered oxidative stress, as indicated by increased activities of antioxidant enzymes (SOD, CAT, and GPx) during the initial 24 hours, signaling an adaptive response. However, prolonged exposure led to a decline in enzyme activities by 48 and 96 hours due to excessive reactive oxygen species (ROS) accumulation. Increased malondialdehyde (MDA) levels indicated significant lipid peroxidation and oxidative damage. Despite partial recovery in enzyme activities after 48 hours of post-exposure recovery, they remained below control levels, highlighting incomplete restoration and lingering oxidative stress. The relationship between oxidative damage, as indicated by malondialdehyde (MDA) levels and histological changes such as necrosis and vacuolation demonstrates the severity and extent of tissue damage over time under ammonia nitrogen (NH$_3$-N) stress. High MDA levels reflect increased lipid peroxidation due to excessive reactive oxygen species (ROS), a hallmark of oxidative stress. This oxidative damage correlates directly with histopathological changes observed in the liver of juvenile four-finger threadfin (*Eleutheronema tetradactylum*). Histologically, the progression of damage starts with early swelling of hepatocytes and nuclear deformation (after 12 hours), advancing to vacuolation and congestion (24 hours), and eventually leading to necrosis, nuclear dissolution, and blurred cell outlines by 48–96

hours. These changes align with persistently higher MDA levels, indicating continuous oxidative membrane damage and compromised cell integrity. The persistence of vacuolation and necrosis after prolonged exposure highlights the insufficiency of antioxidant defenses, as evidenced by declining antioxidant enzyme activities (SOD, CAT, GPx). Even after a 48-hour recovery period, partial alleviation of sinusoidal dilation and hepatocyte vacuolation is accompanied by persistently high MDA levels, underlining incomplete recovery from oxidative stress. Hence, MDA serves as a reliable marker of oxidative damage severity, directly linked to the histological manifestations of liver injury under NH_3-N stress. Although some histological and metabolic functions partially recovered, persistent alterations in nutrient transport and liver metabolism were evident, as confirmed by KEGG pathway analysis. These findings underline the critical need for effective water quality management in aquaculture systems to minimize ammonia toxicity and mitigate its long-term effects on fish health and viability. Further studies on stress resilience mechanisms are essential for improving aquaculture practices and fostering environmental stress tolerance.

Data availability statement

The original contributions presented in the study are included in the article/supplementary material. Further inquiries can be directed to the corresponding author.

Ethics statement

The use of all animals in this project was conducted under the Animal Welfare Act, the PHS Animal Welfare Policy, the National Institutes of Health (NIH) Guide for Care and Use of Laboratory Animals, and the policies and procedures of the People's Republic of China, Guangdong province, and Guangdong Ocean University. The study was conducted in compliance with the regulations for administering laboratory animals in Guangdong province, China, and in compliance with the Guangdong Ocean University Research Council's guidelines for the care and use of laboratory animals (approval number: GDOU-LAE-2023-015).

Author contributions

J-HJ: Data curation, Formal Analysis, Investigation, Methodology, Project administration, Software, Validation, Visualization, Writing – original draft, Writing – review & editing. H-JW: Data curation, Software, Validation, Writing – original draft. EA: Data curation, Formal Analysis, Methodology, Software, Validation, Visualization, Writing – original draft, Writing – review & editing. YL: Data curation, Software, Validation, Writing – original draft. R-TX: Data curation, Resources, Software, Supervision, Writing – original draft. Z-LW: Data curation, Resources, Software, Supervision, Writing – original draft. J-SH: Conceptualization, Funding acquisition, Methodology, Resources, Supervision, Validation, Visualization, Writing – original draft, Writing – review & editing.

Conflict of interest

Author R-TX was employed by the company Guangdong Evergreen Feed Industry Co. Ltd.

The remaining authors declare that the research was conducted without commercial or financial relationships that could be construed as a potential conflict of interest.

The author(s) declared that they were an editorial board member of Frontiers, at the time of submission. This had no impact on the peer review process and the final decision.

Generative AI statement

The author(s) declare that no Generative AI was used in the creation of this manuscript.

Publisher's note

All claims expressed in this article are solely those of the authors and do not necessarily represent those of their affiliated organizations, or those of the publisher, the editors and the reviewers. Any product that may be evaluated in this article, or claim that may be made by its manufacturer, is not guaranteed or endorsed by the publisher.

References

Abbas, H. H. (2006). Acute toxicity of ammonia to common carp fingerlings (*Cyprinus carpio*) at different pH levels. *Pakistan J. Biol. Sci.* 9, 2215–2221. doi: 10.3923/pjbs.2006.2215.2221

Albrecht, J. (2007). "Ammonia toxicity in the central nervous system. In: A. Lajtha, S. S. Oja, A. Schousboe and P. Saransaari (eds) *Handbook of Neurochemistry and Molecular Neurobiology*. New York, NY: Springer. doi: 10.1007/978-0-387-30373-4_12

Andolfo, G., Ruocco, M., Di Donato, A., Frusciante, L., Lorito, M., Scala, F., et al. (2015). Genetic variability and evolutionary diversification of membrane ABC transporters in plants. *BMC Plant Biol.* 15, 1–51. doi: 10.1186/s12870-014-0323-2

Annunziata, M. G., Ciarmiello, L. F., Woodrow, P., and Carillo, P. (2019). Spatial and temporal profile of glycine betaine accumulation in plants under abiotic stresses. *Front. Plant Sci.* 10. doi: 10.3389/fpls.2019.00230

Aranda-Morales, S. A., Peña-Marín, E. S., Jiménez-Martínez, L. D., Martínez-Burguete, T., Martínez-Bautista, G., Álvarez-Villagómez, C. S., et al. (2021). Expression of ion transport proteins and routine metabolism in juveniles of tropical gar (*Atractosteus tropicus*) exposed to ammonia. *Comp. Biochem. Physiol. Part C: Toxicol. Pharmacol.* 250, 109166. doi: 10.1016/j.cbpc.2021.109166

Arief, H., Feliatra, F., Darwis,, and Dewi, N. (2023). Bioeconomic study and optimal use of the fourfinger threadfin (*Eleutheronema tetradactylum*) resource in Rokan Hilir Regency, Riau Province, Indonesia. *AACL Bioflux*. 16, 282–290.

Baliou, S., Kyriakopoulos, A. M., Goulielmaki, M., Panayiotidis, M. I., Spandidos, D. A., and Zoumpourlis, V. (2020). Significance of taurine transporter (TauT) in homeostasis and its layers of regulation. *Mol. Med. Rep.* 22, 2163–2173. doi: 10.3892/mmr.2020.11321

Bănăduc, D., Barinova, S., Lozano, V. L., Afanasyev, S., Leite, T., Branco, P., et al. (2024). Multi-interacting natural and anthropogenic stressors on freshwater ecosystems: their current status and future prospects for 21st century. *Water* 16, 1483. doi: 10.3390/w16111483

Bashir, I., Lone, F. A., Bhat, R. A., Mir, S. A., Dar, Z. A., and Dar, S. A. (2020). Concerns and threats of contamination on aquatic ecosystems. In: K. Hakeem, R. Bhat and H. Qadri (eds) *Bioremediation and Biotechnology*. Springer, Cham. p. 1–26. doi: 10.1007/978-3-030-35691-0_1

Benli, A.Ç.K., Köksal, G., and Özkul, A. (2008). Sublethal ammonia exposure of Nile tilapia (*Oreochromis niloticus* L.): Effects on gill, liver and kidney histology. *Chemosphere* 72, 1355–1358. doi: 10.1016/j.chemosphere.2008.04.037

Bizoń, A., Chojdak-Łukasiewicz, J., Budrewicz, S., Pokryszko-Dragan, A., and Piwowar, A. (2023). Exploring the relationship between antioxidant enzymes, oxidative stress markers, and clinical profile in relapsing–remitting multiple sclerosis. *Antioxidants* 12 (8), 1638. doi: 10.3390/antiox12081638

Camargo, J. A., and Alonso, Á. (2006). Ecological and toxicological effects of inorganic nitrogen pollution in aquatic ecosystems: A global assessment. *Environ. Int.* 32, 831–849. doi: 10.1016/j.envint.2006.05.002

Colares, J. R., Hartmann, R. M., Schemitt, E. G., Fonseca, S. R. B., Brasil, M. S., Picada, J. N., et al. (2021). Melatonin prevents oxidative stress, inflammatory activity, and DNA damage in cirrhotic rats. *World J. Gastroenterol.* 28, 348–364. doi: 10.3748/wjg.v28.i3.348

Du, S. N., Mahalingam, S., Borowiec, B. G., and Scott, G. R. (2016). Mitochondrial physiology and reactive oxygen species production are altered by hypoxia acclimation in killifish (*Fundulus heteroclitus*). *J. Exp. Biol.* 219, 1130–1138. doi: 10.1242/jeb.132860

Edwards, T. M., Puglis, H. J., Kent, D. B., Durán, J. L., Bradshaw, L. M., and Farag, A. M. (2024). Ammonia and aquatic ecosystems – A review of global sources, biogeochemical cycling, and effects on fish. *Sci. Total Environ.* 907, 167911. doi: 10.1016/j.scitotenv.2023.167911

Fortin, É., Blouin, R., Lapointe, J., Petit, H. V., and Palin, M.-F. (2017). Linoleic acid, α-linolenic acid and enterolactone affect lipid oxidation and expression of lipid metabolism and antioxidant-related genes in hepatic tissue of dairy cows. *Br. J. Nutr.* 117, 1199–1211. doi: 10.1017/S0007114517000976

Furumoto, H., Nanthirudjanar, T., Kume, T., Izumi, Y., Park, S., Kitamura, N., et al. (2016). 10-Oxo-trans-11-octadecenoic acid generated from linoleic acid by a gut lactic acid bacterium *Lactobacillus plantarum* is cytoprotective against oxidative stress. *Toxicol. Appl. Pharmacol.* 296, 1–9. doi: 10.1016/j.taap.2016.02.012

Gao, J., Du, F., Gu, R., and Xu, G. (2015). Effect of transport stress on physiological-biochemical indices and expression of HPI genes and roles of glycyrrhizin on transport response in *Coilia nasus*. *J. Shanghai Ocean Univ.* 24, 817–825.

Gao, X., Fei, F., Huang, B., Meng, X. S., Zhang, T., Zhao, K., et al. (2021). Alterations in hematological and biochemical parameters, oxidative stress, and immune response in *Takifugu rubripes* under acute ammonia exposure. *Comp. Biochem. Physiol. Part C: Toxicol. Pharmacol.* 243, 108978. doi: 10.1016/j.cbpc.2021.108978

Gómez-Virgilio, L., Silva-Lucero, C., Flores-Morelos, S., Gallardo-Nieto, J., Lopez-Toledo, G., Abarca-Fernandez, M., et al. (2022). Autophagy: A key regulator of homeostasis and disease: an overview of molecular mechanisms and modulators. *Cells* 11 (15), 2262. doi: 10.3390/cells11152262

Han, H., Zhou, Y., Liu, Q., Wang, G., Feng, J., and Zhang, M. (2021). Effects of ammonia on gut microbiota and growth performance of broiler chickens. *Animals: Open Access J. From MDPI* 11 (6), 1716. doi: 10.3390/ani11061716

Handy, R. D., and Poxton, M. G. (1993). Nitrogen pollution in mariculture: toxicity and excretion of nitrogenous compounds by marine fish. *Rev. Fish Biol. Fisheries* 3, 205–241. doi: 10.1007/BF00043929

Hao, R., Du, X., Yang, C., Deng, Y., Zheng, Z., and Wang, Q. (2019). Integrated application of transcriptomics and metabolomics provides insights into unsynchronized growth in pearl oyster *Pinctada fucata* martensii. *Sci. Total Environ.* 666, 46–56. doi: 10.1016/j.scitotenv.2019.02.221

Hargreaves, J. A., and Kucuk, S. (2001). Effects of diel un-ionized ammonia fluctuation on juvenile hybrid striped bass, channel catfish, and blue tilapia. *Aquaculture* 195, 163–181. doi: 10.1016/S0044-8486(00)00543-3

Hegazi, M. M., Attia, Z. I., and Ashour, O. A. (2010). Oxidative stress and antioxidant enzymes in liver and white muscle of Nile tilapia juveniles in chronic ammonia exposure. *Aquat. Toxicol.* 99, 118–125. doi: 10.1016/j.aquatox.2010.04.007

Hu, Y., Huang, Y., Zhong, L., Xiao, T.-Y., Wen, H., Huan, Z.-L., et al. (2012). Effects of ammonia stress on the gill Na+/K+-ATPase, microstructure and some serum physiological-biochemical indices of juvenile black carp (*Mylopharyngodon piceus*). *J. Fisheries Of China* 36, 538–545. doi: 10.3724/SP.J.1231.2012.27713

Huang, C. T., Afero, F., Lu, F. Y., Chen, B.-Y., Huang, P.-L., Lan, H.-Y., et al. (2022). Bioeconomic evaluation of *Eleutheronema tetradactylum* farming: a case study in Taiwan. *Fish Sci.* 88, 437–447. doi: 10.1007/s12562-022-01591-4

Ip, Y. K., and Chew, S. F. (2010). Ammonia production, excretion, toxicity, and defense in fish: A review. *Front. Physiol.* 1. doi: 10.3389/fphys.2010.00134

Iqbal, T. H., Hajisamae, S., Lim, A., Jantarat, S., Wang, W., and Tsim, K. W. K. (2023). Feeding habits of four-finger threadfin fish, *Eleutheronema tetradactylum*, and its diet interaction with co-existing fish species in the coastal waters of Thailand. *PeerJ* 11, e14688. doi: 10.7717/peerj.14688

Jin, J., Amenyogbe, E., Yang, Y., Wang, Z., Lu, Y., Xie, R., et al. (2024). Effects of ammonia nitrogen stress on the physiological, biochemical, and metabolic levels of the gill tissue of juvenile four-finger threadfin (*Eleutheronema tetradactylum*). *Aquat. Toxicol.* 274, 107049. doi: 10.1016/j.aquatox.2024.107049

Katsiadaki, I., Ellis, T., Andersen, L., Antczak, P., Blaker, E., Burden, N., et al. (2021). Dying for change: A roadmap to refine the fish acute toxicity test after 40 years of applying a lethal endpoint. *Ecotoxicology Environ. Saf.* 223, 112585. doi: 10.1016/j.ecoenv.2021.112585

Konger, R. L., Marathe, G. K., Yao, Y., Zhang, Q., and Travers, J. B. (2008). Oxidized glycerophosphocholines as biologically active mediators for ultraviolet radiation-mediated effects. *Prostaglandins Other Lipid Mediators* 87, 1–8. doi: 10.1016/j.prostaglandins.2008.04.002

Kullgren, A., Jutfelt, F., Fontanillas, R., Sundell, K., Samuelsson, L., Wiklander, K., et al. (2013). The impact of temperature on the metabolome and endocrine metabolic signals in Atlantic salmon (*Salmo salar*). *Comp. Biochem. Physiol. Part A: Mol. Integr. Physiol.* 164, 44–53. doi: 10.1016/j.cbpa.2012.10.005

Lane, A. N., and Fan, T. W. (2015). Regulation of mammalian nucleotide metabolism and biosynthesis. *Nucleic Acids Res.* 43, 2466–2485. doi: 10.1093/nar/gkv047

Lee, M., Park, J. C., and Lee, J. (2018). Effects of environmental stressors on lipid metabolism in aquatic invertebrates. *Aquat. Toxicol.* 200, 83–92. doi: 10.1016/j.aquatox.2018.04.016

Li, M., Gong, S., Li, Q., Yuan, L., Meng, F., and Wang, R. (2016). Ammonia toxicity induces glutamine accumulation, oxidative stress and immunosuppression in juvenile yellow catfish *Pelteobagrus fulvidraco*. *Comp. Biochem. Physiol. Part C: Toxicol. Pharmacol.* 183-184, 1–6. doi: 10.1016/j.cbpc.2016.01.005

Li, S., Tan, Y., Wang, N., Zhang, J., Lao, L., Wong, W., et al. (2015). The role of oxidative stress and antioxidants in liver diseases. *Int. J. Mol. Sci.* 16, 26087–26124. doi: 10.3390/ijms161125942

Lin, W., Luo, H., Wu, J., Hung, T., Cao, B., Liu, X., et al. (2022). A review of the emerging risks of acute ammonia nitrogen toxicity to aquatic decapod crustaceans. *Water* 15, 27. doi: 10.3390/w15010027

Liu, Y., Ding, W.-D., Cao, Z.-M., Bing, X.-W., Xu, C., Yang, F., et al. (2019). Effects of acute ammonia nitrogen stress on antioxidant enzymes activity and gene expression involved in inflammation of juvenile *Siniperca chuatsi*. *J. South. Agric.*, 1860–1868.

Liu, M., Guo, H., Zhu, K., Liu, B., Liu, B., Guo, L., et al. (2021). Effects of acute ammonia exposure and recovery on the antioxidant response and expression of genes in the Nrf2-Keap1 signaling pathway in the juvenile golden pompano (*Trachinotus ovatus*). *Aquat. Toxicol.* 240, 105969. doi: 10.1016/j.aquatox.2021.105969

Liu, F., Li, S., Yu, Y., Sun, M., Xiang, J., and Li, F. (2020). Effects of ammonia stress on the hemocytes of the Pacific white shrimp *Litopenaeus vannamei*. *Chemosphere* 239, 124759. doi: 10.1016/j.chemosphere.2019.124759

Liu, J., Qu, W., and Kadiiska, M. B. (2009). Role of oxidative stress in cadmium toxicity and carcinogenesis. *Toxicol. Appl. Pharmacol.* 238, 209–214. doi: 10.1016/j.taap.2009.01.029

Mishra, A. K., and Mohanty, B. (2008). Acute toxicity impacts of hexavalent chromium on behavior and histopathology of gill, kidney and liver of the freshwater fish, *Channa punctatus* (Bloch). *Environ. Toxicol. Pharmacol.* 26, 136–141. doi: 10.1016/j.etap.2008.02.010

Mohiuddin, S. S., and Khattar, D. (2023). Biochemistry, Ammonia. In: *StatPearls* [Internet]. (Treasure Island (FL): StatPearls Publishing). Available online at: https://www.ncbi.nlm.nih.gov/books/NBK541039/ (Accessed February 20, 2023).

Molines, A. T., Lemière, J., Gazzola, M., Steinmark, I. E., Edrington, C. H., Hsu, C., et al. (2022). Physical properties of the cytoplasm modulate the rates of microtubule polymerization and depolymerization. *Dev. Cell* 57, 466–479.e6. doi: 10.1016/j.devcel.2022.02.001

Ngo, V., and Duennwald, M. L. (2022). Nrf2 and oxidative stress: A general overview of mechanisms and implications in human disease. *Antioxidants* 11, 2345. doi: 10.3390/antiox11122345

Ou, Y. (2017). Research on the initial sexual maturity and large-scale breeding technology of four-fingered threadfin broodstock in ponds in Guangdong. *South. Fisheries Sci.* 13, 97–104.

Paust, L. O., Foss, A., and Imsland, A. K. (2011). Effects of chronic and periodic exposure to ammonia on growth, food conversion efficiency and blood physiology in juvenile Atlantic halibut (*Hippoglossus hippoglossus* L.). *Aquaculture* 315, 400–406. doi: 10.1016/j.aquaculture.2011.03.008

Pramanik, S., and Biswas, J. K. (2024). Histopathological fingerprints and biochemical changes as multi-stress biomarkers in fish confronting concurrent pollution and parasitization. *IScience* 27, 111432. doi: 10.1016/j.isci.2024.111432

Qiang, J., Xu, P., and He, J. (2011). The combined effects of external ammonia and crowding stress on growth and biochemical activities in liver of (GIFT) Nile tilapia juvenile (*Oreochromis niloticus*). *J. Fisheries China* 35, 1837–1848.

Qiu, L., Shi, X., Yu, S., Han, Q., Diao, X., and Zhou, H. (2018). Changes of ammonia-metabolizing enzyme activity and gene expression of two strains in shrimp *litopenaeus vannamei* under ammonia stress. *Front. Physiol.* 9. doi: 10.3389/fphys.2018.00211

Qu, Z., Nong, W., Yu, Y., Baril, T., Yip, H. Y., Hayward, A., et al. (2020). Genome of the four-finger threadfin *Eleutheronema tetradactylum* (Perciforms: Polynemidae). *BMC Genomics* 21 (1), 726. doi: 10.1186/s12864-020-07145-1

Rainboth, W. J. (1996). *Fishes of the Cambodian mekong* (Rome: Food & Agriculture Org).

Rébeillé, F., Ravanel, S., Marquet, A., Mendel, R. R., Webb, M. E., Smith, A. G., et al. (2007). Roles of vitamins B5, B8, B9, B12 and molybdenum cofactor at cellular and organismal levels. *Natural product Rep.* 24, 949–962. doi: 10.1039/b703104c

Ren, Q., and Pan, L. (2014). Digital gene expression analysis in the gills of the swimming crab (*Portunus trituberculatus*) exposed to elevated ambient ammonia-N. *Aquaculture* 434, 108–114. doi: 10.1016/j.aquaculture.2014.08.008

Ruiz-Picos, R. A., Diaz, J. A. R., and López-López, E. (2015). "Histopathological indicators in fish for assessing environmental stress," in *Fish and water quality* (Springer), 1–15. doi: 10.1007/978-94-017-9499-2_38

Sahu, R. P., Turner, M. J., DaSilva, S. C., Rashid, B. M., Ocana, J. A., Perkins, S. M., et al. (2012). The environmental stressor ultraviolet B radiation inhibits murine antitumor immunity through its ability to generate platelet-activating factor agonists. *Carcinogenesis* 33, 1360–1367. doi: 10.1093/carcin/bgs152

Sinha, A. K., Zinta, G., AbdElgawad, H., Asard, H., Blust, R., and De Boeck, G. (2015). High environmental ammonia elicits differential oxidative stress and antioxidant responses in five different organs of a model estuarine teleost (*Dicentrarchus labrax*). *Comp. Biochem. Physiol. Part C: Toxicol. Pharmacol.* 174-175, 21–31. doi: 10.1016/j.cbpc.2015.06.002

Smith, C. A., Want, E. J., O'Maille, G., Abagyan, R., and Siuzdak, G. (2006). XCMS: processing mass spectrometry data for metabolite profiling using nonlinear peak alignment, matching, and identification. *Analytical Chem.* 78, 779–787. doi: 10.1021/ac051437y

Sokolova, I. M., Frederich, M., Bagwe, R., Lannig, G., and Sukhotin, A. A. (2012). Energy homeostasis as an integrative tool for assessing limits of environmental stress tolerance in aquatic invertebrates. *Mar. Environ. Res.* 79, 1–15. doi: 10.1016/j.marenvres.2012.04.003

Sun, Y., Fu, Z., and Ma, Z. (2024). The effects of acute ammonia stress on liver antioxidant, immune and metabolic responses of juvenile yellowfin tuna (*Thunnus albacares*). *Comp. Biochem. Physiol. Part A: Mol. Integr. Physiol.* 297, 111707. doi: 10.1016/j.cbpa.2024.111707

Wang, Z., Chen, S., Cao, D., Lu, B., Chang, Q., Liu, C., et al. (2017). Effects of acute ammonia nitrogen stress on histopathology of gill and liver and enzyme activities of juvenile *verasper variegatus*. *Prog. Fishery Sci.* 38, 59–69.

Wen, J.-F., Lan, J.-N., Zhou, H., Wang, P.-F., Ou, Y.-J., and Li, J.-E. (2019). Effects of different salinities on histological structure of digestive organs of juvenile *Lateolabrax maculatus*. *J. South. Agric.* 50, 2826–2832.

Wilkens, S. (2015). Structure and mechanism of ABC transporters. *F1000Prime Rep.* 7, 14. doi: 10.12703/P7-14

Winston, J. A., and Theriot, C. M. (2020). Diversification of host bile acids by members of the gut microbiota. *Gut Microbes* 11, 158–171. doi: 10.1080/19490976.2019.1674124

Wu, X. (2008). Mechanisms and assessment of water eutrophication. *J. Zhejiang University. Science. B* 9, 197. doi: 10.1631/jzus.B0710626

Xu, Z., Cao, J., Qin, X., Qiu, W., Mei, J., and Xie, J. (2021). Toxic effects on bioaccumulation, hematological parameters, oxidative stress, immune responses and tissue structure in fish exposed to ammonia nitrogen: A review. *Animals* 11, 3304. doi: 10.3390/ani11113304

Xu, W., Li, H., Wu, L., Jin, J., Han, D., Zhu, X., et al. (2022). Taurine Alleviates Cadmium-Induced Toxicity via Genetically Specific Strategies in Two Strains of Gibel Carp (*Carassius gibelio*). *Antioxidants* 11, 1381. doi: 10.3390/antiox11071381

Yan, S., Meng, Z., Tian, S., Teng, M., Yan, J., Jia, M., et al. (2020). Neonicotinoid insecticides exposure cause amino acid metabolism disorders, lipid accumulation and oxidative stress in ICR mice. *Chemosphere* 246, 125661. doi: 10.1016/j.chemosphere.2019.125661

Yan, Z., Wan, J., Liu, J., Yao, B., Lu, Y., Guo, Z., et al. (2023). [amp]]alpha;-lipoic acid ameliorates hepatotoxicity induced by chronic ammonia toxicity in crucian carp (*Carassius auratus gibelio*) by alleviating oxidative stress, inflammation and inhibiting ERS pathway. *Ecotoxicology Environ. Saf.* 266, 115533. doi: 10.1016/j.ecoenv.2023.115533

Yang, E., Amenyogbe, E., Zhang, J., Wang, W., Huang, J., and Chen, G. (2022). Integrated transcriptomics and metabolomics analysis of the intestine of cobia (*Rachycentron canadum*) under hypoxia stress. *Aquaculture Rep.* 25, 101261. doi: 10.1016/j.aqrep.2022.101261

Yang, X., Ye, J., Zhou, Z.-J., Zhang, Y.-X., Wu, C.-L., and Ming, J.-H. (2014). Study on the optimal levels of dietary leucine and isoleucine for juvenile Chinese mitten crabs, Eriocheir sinensis. *Acta Hydrobiologica Sin.* 38, 1062–1070. doi: 10.7541/2014.156

Yang, K., Zhong, Q., Qin, H., Long, Y., Ou, H., Ye, J., et al. (2020). Molecular response mechanism in Escherichia coli under hexabromocyclododecane stress. *Sci. Total Environ.* 708, 135199. doi: 10.1016/j.scitotenv.2019.135199

Ye, H., Xiao, S., Wang, X., Wang, Z., Zhang, Z., Zhu, C., et al. (2018). Characterization of Spleen Transcriptome of Schizothorax prenanti during *Aeromonas hydrophila* Infection. *Mar. Biotechnol.* 20, 246–256. doi: 10.1007/s10126-018-9801-0

Yoon, H., Shaw, J. L., Haigis, M. C., and Greka, A. (2021). Lipid metabolism in sickness and in health: Emerging regulators of lipotoxicity. *Mol. Cell* 81, 3708. doi: 10.1016/j.molcel.2021.08.027

Zeng, X., Liu, R., Li, Y., Li, J., Zhao, Q., Li, X., et al. (2021). Excessive ammonia inhalation causes liver damage and dysfunction by altering gene networks associated with oxidative stress and immune function. *Ecotoxicology Environ. Saf.* 217, 112203. doi: 10.1016/j.ecoenv.2021.112203

Zhang, Y., Chen, R., Zhang, D., Qi, S., and Liu, Y. (2023). Metabolite interactions between host and microbiota during health and disease: Which feeds the other? *Biomedicine Pharmacotherapy* 160, 114295. doi: 10.1016/j.biopha.2023.114295

Zhang, L., Nawata, C. M., and Wood, C. M. (2013). Sensitivity of ventilation and brain metabolism to ammonia exposure in rainbow trout, Oncorhynchus mykiss. *J. Exp. Biol.* 216, 4025–4037. doi: 10.1242/jeb.087692

Zhang, W., Sun, S., Ge, X., Zhu, J., Li, B., Miao, L.-H., et al. (2015). Acute effects of ammonia exposure on histopathology of gill, liver and kidney in juvenile *Megalobrama amblycephala* and the post-exposure recovery. *J. Fisheries China* 39, 233–244.

Zhang, W., Xia, S., Zhu, J., Miao, L., Ren, M., Lin, Y., et al. (2019). Growth performance, physiological response and histology changes of juvenile blunt snout bream, *Megalobrama amblycephala* exposed to chronic ammonia. *Aquaculture* 506, 424–436. doi: 10.1016/j.aquaculture.2019.03.072

Zhang, L., Xu, E. G., Li, Y., Liu, H., Vidal-Dorsch, D. E., and Giesy, J. P. (2018). Ecological risks posed by ammonia nitrogen (AN) and un-ionized ammonia (NH3) in seven major river systems of China. *Chemosphere* 202, 136–144. doi: 10.1016/j.chemosphere.2018.03.098

Zhang, L., Zhao, G., and Fan, X. (2016). Effects of ammonia on growth, digestion and antioxidant capacity in juvenile yellow catfish *Pelteobagrus fulvidraco* (Richardson 1846). *J. Appl. Ichthyology* 32, 1205–1212. doi: 10.1111/jai.13203

Zhao, M., Yao, D., Li, S., Zhang, Y., and Aweya, J. J. (2020). Effects of ammonia on shrimp physiology and immunity: A review. *Rev. Aquaculture* 12, 2194–2211. doi: 10.1111/raq.12429

Zheng, H.-W., Yang, S.-Q., and Sun, Y. (2020). Effects of exposure to acute ammonia nitrogen stress on ACP, CAT and MDA of juvenile *macropterus salmoides*. *J. Zhejiang Ocean Univ. (Natural Science)* 39, 27–33.

Zhou, L., and Boyd, C. E. (2015). An assessment of total ammonia nitrogen concentration in Alabama (USA) ictalurid catfish ponds and the possible risk of ammonia toxicity. *Aquaculture* 437, 263–269. doi: 10.1016/j.aquaculture.2014.12.001

Zhou, J., Liu, C., Yang, Y., Yang, Y., Gu, Z., Wang, A., et al. (2023). Effects of long-term exposure to ammonia on growth performance, immune response, and body biochemical composition of juvenile ivory shell, *Babylonia areolata*. *Aquaculture* 562, 738857. doi: 10.1016/j.aquaculture.2022.738857